Efficient Hybrid TLM/Mode-Matching Analysis of Packaged Components

Mario Righi, *Member, IEEE*, Jonathan L. Herring, and Wolfgang J. R. Hoefer, *Fellow, IEEE*

***Abstract*— A combination of the transmission-line matrix (TLM) method and time-domain mode-matching method is proposed. The resulting hybrid algorithm takes full advantage of time-domain methods for regions with highly complex geometries while exploiting the efficiency of analytical formulations for the more regular regions. The computational aspects and the errors involved in the procedure are investigated. The approach is demonstrated with the analysis of a packaged microstrip line containing a via-hole, and results are compared with independent measurements. While the planar circuit is discretized by a TLM mesh, the field in the package is decomposed into modal fields. The two sub-domains are joined by modal diakoptics. Thus, we obtain not only a significant reduction in computer time and memory, but also gain new physical insight into the physics of package resonance.**

***Index Terms*— Mode-matching methods, packaging, transmission-line matrix methods.**

I. Introduction

THE use of shields around microwave components is becoming increasingly important in order to protect the circuit from harmful environments and to satisfy electromagnetic compatibility (EMC) and electromagnetic interference (EMI) requirements [1]. The effect of the package and its interaction with the circuit it shields is extremely important since the package resonances may drastically change the performance of the circuit. In some cases, the package resonances may be exploited and incorporated into the design of the complete circuit to be used as an additional filter [2].

The full-wave analysis of such a problem is complicated by the complex geometry under study. The transition from the input coaxial line to the planar circuit, the planar circuit itself and the transition to the output coaxial line, are all discontinuities which must be considered when studying their interaction with the package. Fully numerical methods, such as the transmission-line matrix (TLM) [3], and finite-difference time-domain (FDTD) method [4] allow the global analysis of the structure including transitions, planar circuit, and the package, and are thus, ideal methods for the solution of such structures. In addition, their time-domain capabilities allow transient analysis as well as the inclusion of nonlinear and time-varying components inside the package. However, it is necessary to discretize the entire structure, which often leads to a heavy computational load. Alternatively, semianalytical methods can take advantage of *a priori* knowledge of a structure in order to generate efficient, but geometry-specific, algorithms. A hybrid solution can describe uniform subvolumes in analytical form while discretizing more complex subsections for numerical treatment [5].

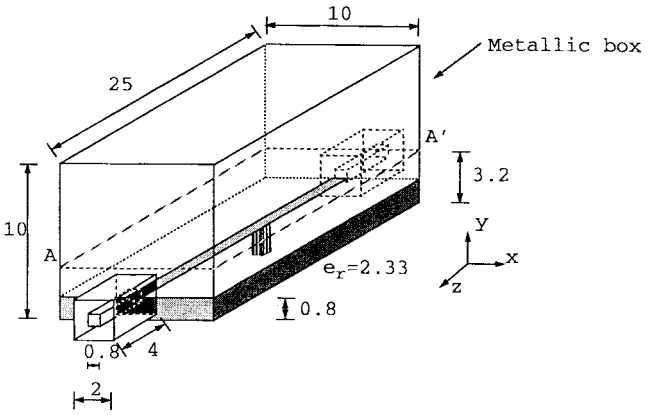

Fig. 1. Geometry of a packaged microstrip via-hole (including coax-to-microstrip transitions) [6]. Square coaxial characteristic impedance 50 Ω, microstrip characteristic impedance 50.5 Ω, via-hole size: 0.8 × 0.8 mm. All other dimensions in the figure are in mm.

For the structure shown in Fig. 1 [6], most of the computational space enclosed by the package is empty. Such situations are particularly suitable for a hybrid procedure. If the package is of regular shape, a modal approach can be applied [7]–[9].

II. Theory

In time-domain diakoptics, a sub-volume is characterized at one or more reference planes by its time-domain impulse response. In general, each reference plane intersects many cells in the cross section and the ports on each of these cells must be terminated in an appropriate manner. A cell-to-cell interaction would be computationally intensive, but in the case of uniform waveguide sections with frequency independent-mode configuration, a more compact representation of the electromagnetic field is offered by a representation of the field in terms of modal basis functions. Once a modal decomposition is performed, each of the modal transmission lines is uncoupled from the others (for uniform sections) thus reducing the complexity of that portion of the structure. Several ways

Manuscript received October 29, 1996; revised June 20, 1997. This work was supported by the Natural Sciences and Engineering Research Council of Canada, by the Science Council of British Columbia, MPR Teltech, Inc. of Burnaby, B.C., and by the University of Victoria.

M. Righi and W. J. R. Hoefer are with the Department of Electrical and Computer Engineering, University of Victoria, Victoria, B.C., V8W 3P6 Canada.

J. L. Herring was with the Department of Electrical and Computer Engineering, University of Victoria, Victoria, B.C., V8W 3P6 Canada. He is now with Schumberger GeoQuest, Abingdon, 0X1 1ND U.K.

Publisher Item Identifier S 0018-9480(97)07106-8.

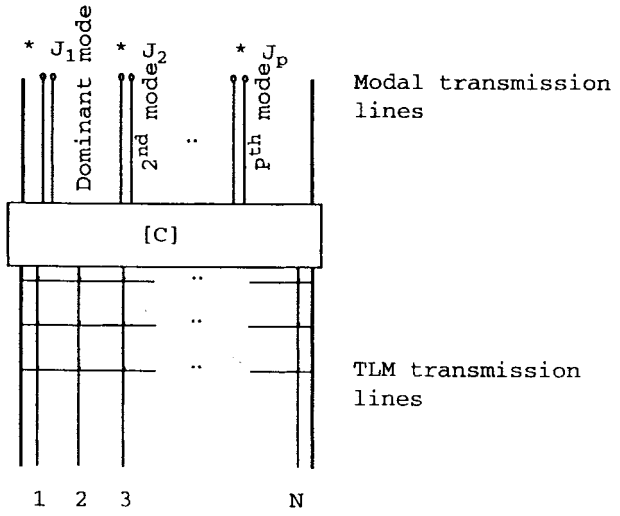

Fig. 2. Discrete spatial Fourier transformer represented by the coupling matrix $[C]$.

of applying a modal approach to the TLM and FDTD method have been proposed.

The first way involves pre-computing, either numerically or analytically, the time-domain modal-impulse response of the portion of waveguide of interest. While in the frequency domain, the reconnection process is performed by multiplying the incident wave with the reflection coefficient of that one-port, it requires in the time domain the convolution of the incident wave with the impulse response of the same element. This procedure has been used successfully in the TLM [10], [11] and FDTD method [12]–[14].

More recently, an alternative approach has been proposed [15] for the FDTD method in which each modal transmission line is modeled with an independent one-dimensional (1-D) FDTD algorithm. This amounts to computing the convolution as the simulation proceeds.

In both cases, a three-dimensional (3-D) problem is reduced to a number of 1-D problems.

In this paper, we make use of the first approach. The essential steps are outlined below.

1) A transformer is first introduced to convert the electromagnetic field from a TLM representation to a mode representation, as shown in Fig. 2. The coupling matrix $[C]$ is computed only once at the beginning of the procedure. Its elements are computed based on a knowledge of the modal field distribution and on the discretization used:

$$C_{mn,ij} = \int_S \Pi_{ij}(\mathbf{r}')\Phi_{mn}(\mathbf{r}')\,d\mathbf{r}' \tag{1}$$

where $\Phi_{mn}(\mathbf{r})$ is the mode eigenfunction, the integration domain S is the waveguide cross section, and $\Pi_{ij}(\mathbf{r})$ is the TLM impulse basis function [16]. In the TLM method, the link–line voltages are a linear combination of the electromagnetic fields. This allows us to operate directly on the voltage pulses rather than first extracting the equivalent fields.

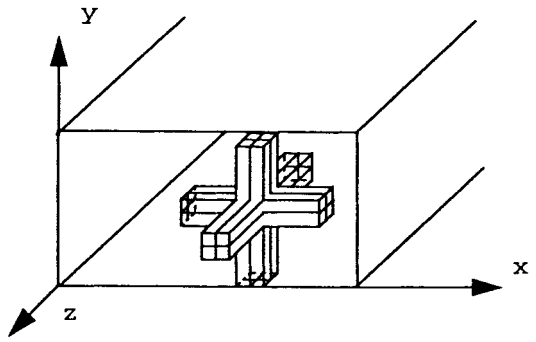

Fig. 3. Homogenous waveguide section discretized with a mesh of 3-D symmetrical condensed node (SCN)–TLM nodes.

2) The voltages incident on the interface plane at time $t = k\Delta t$ are represented in terms of a sum of modes, each with amplitude $A_m^i(k)$ given by

$$[A^i(k)] = [C]^T\,[V^i(k)]. \tag{2}$$

3) Each modal transmission line is now excited with an incident time-domain waveform given by $A_m^i(k)$. The reflected wave is given by the convolution of the incident wave with the modal impulse response $J(k)$:

$$A_m^r(k) = J(k) * A_m^i(k - k'). \tag{3}$$

4) The reflected mode amplitudes are then superimposed, sampled, and re-injected into the TLM mesh

$$[V^r(k)] = [C]\,[A_m^r(k)]. \tag{4}$$

5) The whole process can be described in compact form as follows:

$$[V^r(k)] = [C]\,[J(k')] * [C]^T\,[V^i(k - k')] \tag{5}$$

where the link–line voltages have been gathered in the arrays $[V^i(k)]$ and $[V^r(k)]$. The time-domain modal Green's functions contained in the matrix $[J]$ can be precomputed by a separate TLM simulation, or, more efficiently, they can be analytically generated. The choice in the number of modes depends on the distance of the reference planes from the closest discontinuity and on the spectrum of the excitation.

Modal decomposition and synthesis is performed over a plane, and therefore, the complexity is proportional to the number of nodes in the cross section and the number of modes included in the boundary conditions (BC's). The complexity involved in each convolution is proportional to the length of the modal discrete time-domain Green's function. For the hybrid approach to be advantageous, the computational effort required for the interface connecting the two sub-volumes must be less than that required to simulate the sub-volume represented by the interface. The approach becomes more attractive as the size of this sub-volume increases.

III. Generation of Analytical Modal Time-Domain Green's Functions

For the rectangular waveguide cross section shown in Fig. 3 and modeled with the symmetrical condensed node, there are two voltage pulses: V_y and V_x, for the vertical and horizontal polarizations.

To generate the modal time-domain Green's functions analytically, the incident and reflected voltage waves for both polarizations must be related through the time-domain modal-impulse responses at the termination. For example, for specific TE_{mn} and TM_{mn} modes simultaneously incident upon the reference plane at time instant t with amplitudes A^i_{TE} and A^i_{TM}, respectively, the horizontal electric-field component is given by

$$E^i_x = \left(-\frac{jk_zk_x}{k_c^2}\,A^i_{\mathrm{TM}} + \frac{j\omega\mu k_y}{k_c^2}\,A^i_{\mathrm{TE}}\right)\cos\left(\frac{m\pi x}{a}\right) \times \sin\left(\frac{n\pi y}{b}\right). \tag{6}$$

Similar expressions are obtained for the other components. The corresponding spatial variations in the link–line voltage pulses are given by [3]

$$\begin{aligned} V^i_y(x,y,t) &= \frac{\Delta 1}{2}\left[E_y(t) - Z_oH_x(t)\right] \\ &= \frac{\Delta 1}{2}\,\sin\left(\frac{m\pi x}{a}\right)\cos\left(\frac{n\pi y}{b}\right) \\ &\quad\times\left\{-\frac{jk_zk_y}{k_c^2}\,A^i_{\mathrm{TM}}(t) - \frac{j\omega\mu k_x}{k_c^2}\,A^i_{\mathrm{TE}}(t)\right. \\ &\quad\left. - Z_o\left[\frac{jk_zk_x}{k_c^2}\,A^i_{\mathrm{TE}}(t) + \frac{j\omega\varepsilon k_y}{k_c^2}\,A^i_{\mathrm{TM}}(t)\right]\right\} \\ &= A^i_y(t)\,\sin\left(\frac{m\pi x}{a}\right)\cos\left(\frac{n\pi y}{b}\right) \end{aligned} \tag{7}$$

$$\begin{aligned} V^i_x(x,y,t) &= \frac{\Delta 1}{2}\left[E_x(t) + Z_oH_y(t)\right] \\ &= \frac{\Delta 1}{2}\,\cos\left(\frac{m\pi x}{a}\right)\sin\left(\frac{n\pi y}{b}\right) \\ &\quad\times\left\{-\frac{jk_zk_x}{k_c^2}\,A^i_{\mathrm{TM}}(t) + \frac{j\omega\mu k_y}{k_c^2}\,A^i_{\mathrm{TE}}(t)\right. \\ &\quad\left. + Z_o\left[\frac{jk_zk_y}{k_c^2}\,A^i_{\mathrm{TE}}(t) - \frac{j\omega\varepsilon k_x}{k_c^2}\,A^i_{\mathrm{TM}}(t)\right]\right\} \\ &= A^i_x(t)\,\cos\left(\frac{m\pi x}{a}\right)\sin\left(\frac{n\pi y}{b}\right) \end{aligned} \tag{8}$$

where A^i_y and A^i_x are the amplitudes of the voltage-mode configuration. Solving (7) and (8) for the TE- and TM-field amplitudes give

$$A^i_{\mathrm{TE}} = \frac{2(k_yA^i_x - k_xA^i_y)}{j\Delta 1(\omega\mu + k_zZ_o)} \tag{9}$$

$$A^i_{\mathrm{TM}} = \frac{-2(k_xA^i_x - k_yA^i_y)}{j\Delta 1(\omega\varepsilon Z_o + k_z)}. \tag{10}$$

Since the termination does not couple modes, the incident TE and TM modes can be terminated with the wave impedances Z_{TE}, and Z_{TM}, respectively. For the TLM voltage pulses on link–lines with real impedance Z_0, a nonzero frequency-dependent reflection coefficient must be applied:

$$A^r_{\mathrm{TE}} = \Gamma_{\mathrm{TE}}(\omega)A^i_{\mathrm{TE}} = \frac{Z_{\mathrm{TE}}(\omega) - Z_0}{Z_{\mathrm{TE}}(\omega) + Z_0}\,A^i_{\mathrm{TE}} \tag{11}$$

$$A^r_{\mathrm{TM}} = \Gamma_{\mathrm{TM}}(\omega)A^i_{\mathrm{TM}} = \frac{Z_{\mathrm{TM}}(\omega) - Z_0}{Z_{\mathrm{TM}}(\omega) + Z_0}\,A^i_{\mathrm{TM}}. \tag{12}$$

The reflected-mode field amplitude is transformed back into the reflected-mode voltage-mode amplitude by means of (7) and (8) written for the reflected, rather that for the incident, wave. The complete transformation from the incident-mode voltages to the reflected-mode voltages in the frequency domain becomes (13), shown at the bottom of the page, from which the corresponding time-domain expressions can be obtained through an inverse Fourier transform (IFT) as follows:

$$\begin{bmatrix} A^r_y(t) \\ A^r_x(t) \end{bmatrix} = \begin{bmatrix} \chi_{yy}(t') & \chi_{yx}(t') \\ \chi_{xy}(t') & \chi_{xx}(t') \end{bmatrix} * \begin{bmatrix} A^i_y(t-t') \\ A^i_x(t-t') \end{bmatrix} \tag{14}$$

where * denotes convolution. The modal time-domain Green's function for the vertical-to-vertical voltage polarization, $\chi_{yy}(t)$ is

$$\chi_{yy}(t) = F^{-1}[\chi_{yy}(\omega)]. \tag{15}$$

The expressions for the other terms are similar.

The causality of the time-domain signals in the IFT is enforced by imposing symmetry on the magnitude and antisymmetry on the phase of $\chi_{yy}(\omega)$ and the other terms [17].

The convolution process in (14) simultaneously matches the vertically and horizontally polarized voltages. The terminating condition is, therefore, imposed upon all four transverse electromagnetic-field components at the same time, thus improving the performance of the BC. Equation (14) can also be interpreted as the reflection-coefficient matrix of a two-port element (one port consisting of the vertically polarized mode and the other port consisting of the horizontally polarized mode). The cross-modal terms $\chi_{yx}(t)$ and $\chi_{xy}(t)$ are equal, as reciprocity implies.

A similar approach to generate time-domain responses from frequency domain data for two-dimensional (2-D) problems has been used in [18]. In the present approach, the IFT is computed by considering the frequency-domain function as a continuous function rather than a periodic one. The continuous time-domain function is later sampled to obtain the discrete Green's function. For the present application, this approach leads to a more robust algorithm.

The reflection coefficient for TLM voltage waves of any termination which does not couple modes can be directly

$$\begin{bmatrix} A^r_y \\ A^r_x \end{bmatrix} = \begin{bmatrix} \dfrac{\Gamma_{\mathrm{TE}}(\omega)k_x^2 + \Gamma_{\mathrm{TM}}(\omega)k_y^2}{k_c^2} & \dfrac{\{-\Gamma_{\mathrm{TE}}(\omega) + \Gamma_{\mathrm{TM}}(\omega)\}k_xk_y}{k_c^2} \\ \dfrac{\{-\Gamma_{\mathrm{TE}}(\omega) + \Gamma_{\mathrm{TM}}(\omega)\}k_xk_y}{k_c^2} & \dfrac{\Gamma_{\mathrm{TE}}(\omega)k_y^2 + \Gamma_{\mathrm{TM}}(\omega)k_x^2}{k_c^2} \end{bmatrix} \begin{bmatrix} A^i_y \\ A^i_x \end{bmatrix} = \begin{bmatrix} \chi_{yy}(\omega) & \chi_{yx}(\omega) \\ \chi_{xy}(\omega) & \chi_{xx}(\omega) \end{bmatrix} \begin{bmatrix} A^i_y \\ A^i_x \end{bmatrix} \tag{13}$$

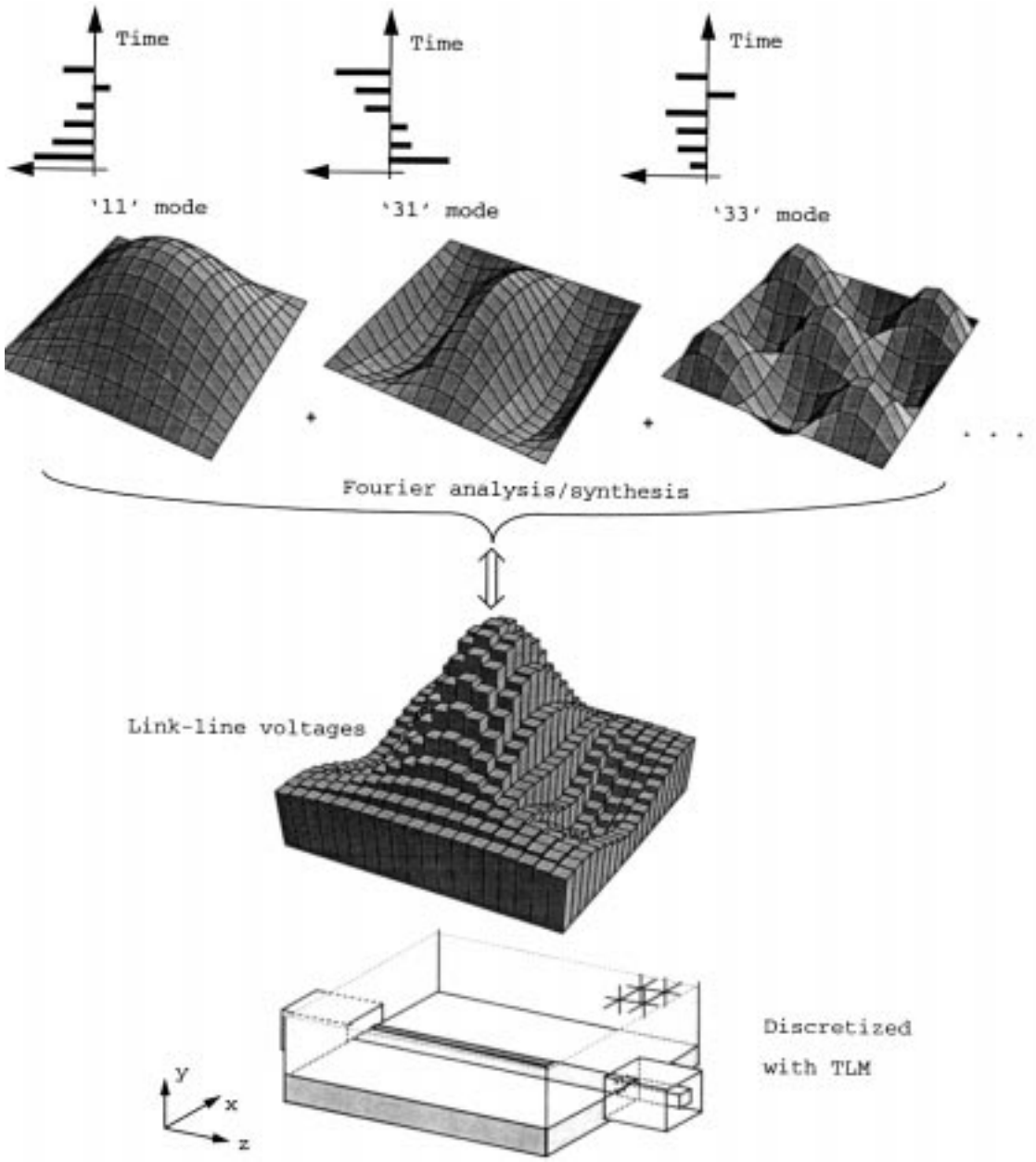

Fig. 4. Segmentation of the structure in Fig. 1 and for the application of the modal approach.

derived from the load it presents to the TE and TM modes. In the case of a termination which does couple modes, (11) and (12) must be written in a matrix form with size consistent with the number of modes coupled. The corresponding time-domain expression in (14) will then become a larger full matrix with elements describing the mode-to-mode time-domain coupling. In this case, the computational load increases, but it still remains much lower than in a full Johns matrix approach [10]. However, it is most efficient to model the discontinuity region (and the way modes are coupled) with the TLM, while analytically describing the adjacent uniform sub-volumes.

The closed-form expressions for the Johns matrix in the frequency domain (13) opens the possibility for further treatment of the Johns stream such as a recursive convolution [19], the use of digital filters [20], or the use of equivalent lumped-element circuits [21], to model the Johns matrix-transfer function. These techniques would lead to a reduced computational load during the convolution process, thus improving the efficiency of the procedure.

IV. Errors Involved in the Modal Approach

The modal approach introduces the following errors: truncation in spacial frequency and truncation in time of the Green's function. The truncation error in spacial frequency arises because the response can take into account only the first P modes excited by the discontinuity. However, it is clear that the significance of the higher order modes on a specific plane is reduced as the distance of the plane from the discontinuity is increased. The finite number of modes taken into account makes the BC's artificially lossy. The choice of the location of the BC's, balanced by the number of

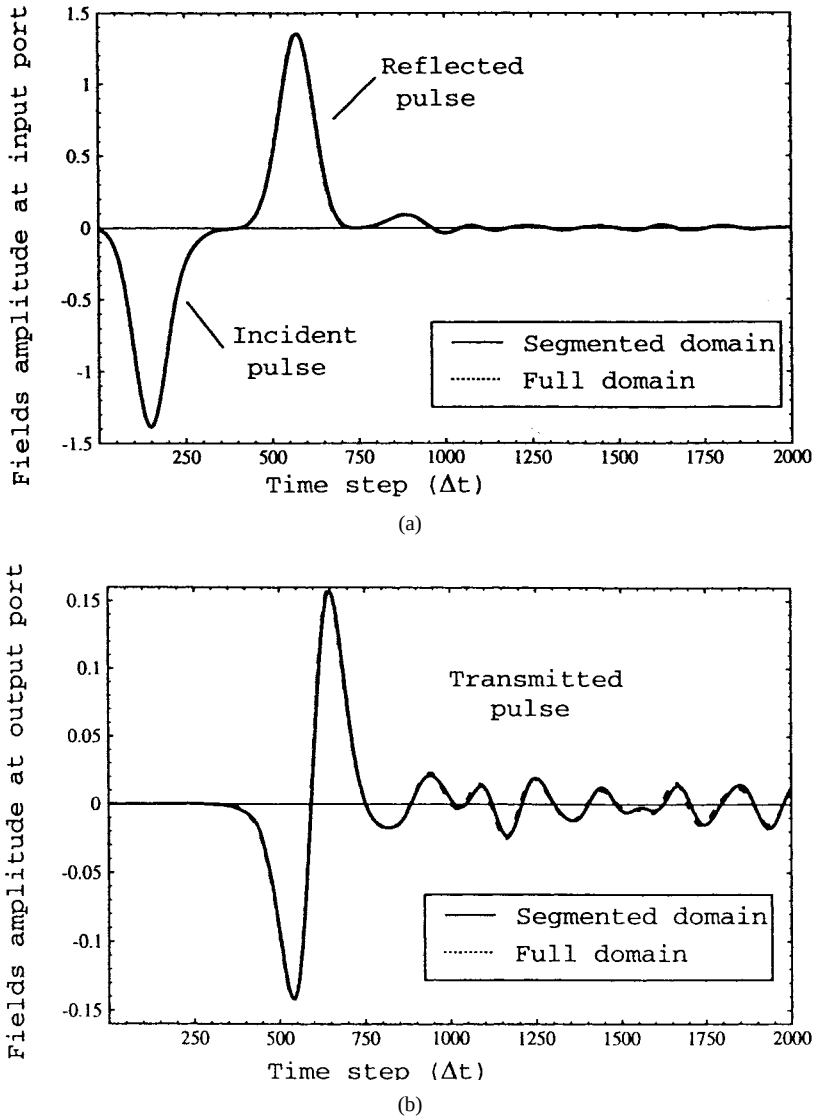

Fig. 5. Time-domain waveforms for the packaged microstrip via-hole. Comparison between the full TLM and the segmented domain results. (a) Signal at the input port and (b) signal at the output port.

modes and the visualization of the amplitude of each mode, ensures that this error is negligible. Another important effect appears when a mode containing significant energy is missed. In this case, the simulation is still stable, but resonances can be suppressed. An extreme case when just three modes are included in the BC's will be shown in the following section.

The truncation error in time occurs because it is often desirable to reduce the computational effort in the convolution by using an impulse response which is shorter than the total simulation time. This means that only the time history covering the last N_t steps of the field penetration into the boundary is taken into account. The late elements of the impulse response are the terms containing the information relative to the frequencies close to the cutoff frequency for that specific mode. Therefore, the truncation of the impulse response worsens the performances of the BC's around these frequencies. The length of the impulse responses must then be such that there is no significant energy remaining.

If the above guidelines are followed, modal diakoptics do not introduce any significant additional error in the frequency range of interest.

V. Application to the Packaged Problem

Previously, the hybrid approach has been used for absorbing BC's (ABC's), where the Green's function represents the time-domain impulse response of a semi-infinite section of waveguide. The performance of modal ABC's approaches the limit of floating point precision, e.g., a return loss of 120 dB in single precision, and 300 dB in double precision.

For this application, we obtain the modal Green's function of a waveguide stub. The short-circuited BC (SBC) differs from the ABC in the following properties: it is not absorbing but purely reactive and it is placed parallel to the propagation direction in the microstrip rather than perpendicular to it.

With reference to Fig. 1, the modal decomposition is performed in the plane AA' [7]. The TLM voltage impulses on this plane represent the near field and the radiated field by the

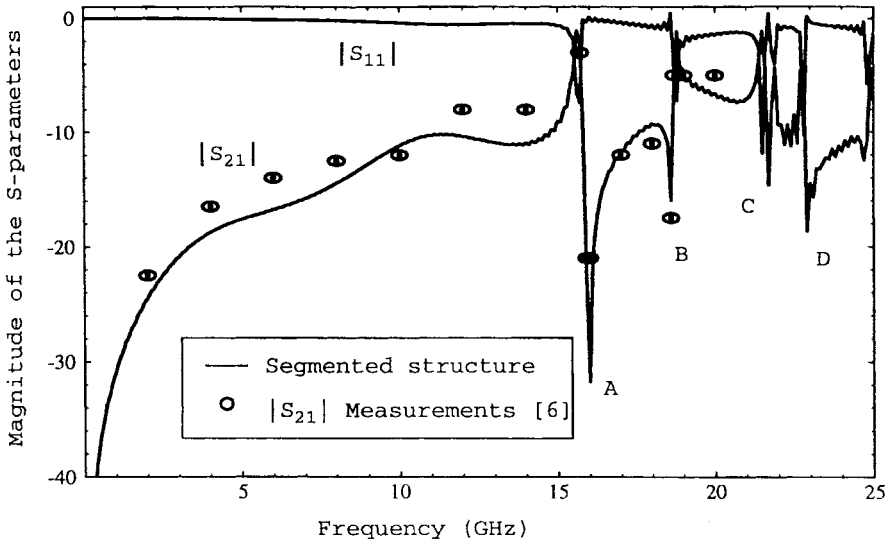

Fig. 6. Magnitude of the S-parameters for the packaged microstrip via-hole (including coax-to-microstrip transitions).

TABLE I
COMPARISON OF MESH SIZE AND CPU TIME FOR THE ANALYSIS OF THE PACKAGED MICROSTRIP VIA-HOLE. SIMULATION WAS PERFORMED FOR 16 000 TIME STEPS

Package	Mesh Size	CPU Time	Memory
Full TLM simulation	25 by 50 by 125	157 min	13 Mbytes
Segmented domain TLM simulation (modes up to TE^y_{43} and TM^y_{43})	25 by 15 by 125	62 min	6 Mbytes

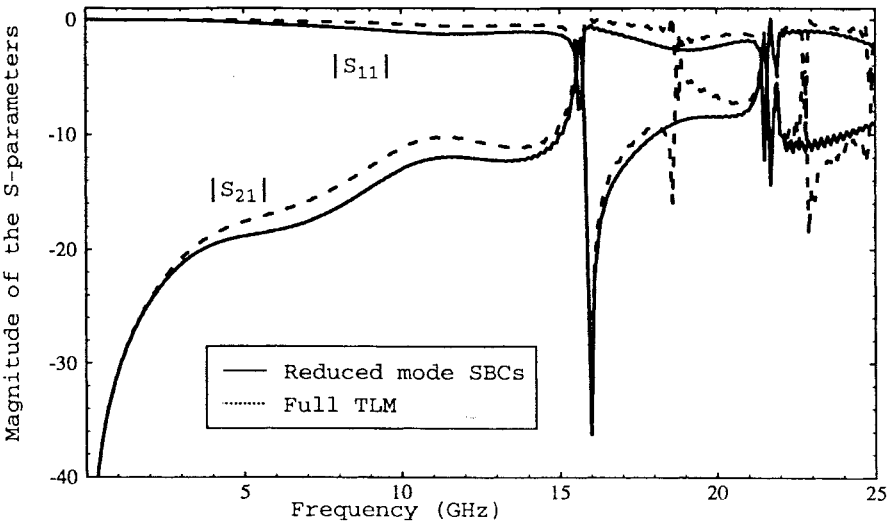

Fig. 7. Magnitude of the S-parameters for the packaged microstrip via-hole (including coax-to-microstrip transitions). Modes up to the "11" order are included.

transitions and the discontinuities of the planar circuit into the package. The field in the xz-plane is decomposed into TE and TM modes with respect to y (TE^y and TM^y).

The modal Green's function of the waveguide stub can be generated analytically or by a separate TLM simulation of that stub. The TLM simulation of a waveguide stub requires the discretization of the whole stub and two separate simulations must be performed for the excitation of the vertical and horizontal voltage pulses. Since there is no coupling between modes, all modes can be processed in these two simulations. The procedure can be computationally intensive for long stubs. On the other hand, the analytical generation of the modal Green's function can be computed by using the stub impedance for the TE and TM modes in (11) and (12), and the computational load does not depend on the length of the stub. The segmentation process is summarized in Fig. 4.

The structure in Fig. 1 is considered as a $2n+2$ port element: two ports are the input and output coaxial lines, while the other $2n$ ports represent n TE and TM modes in the interface AA', which are terminated by multiplying the outgoing waves by the reflection coefficient of the waveguide stub. Modal diakoptics allows the same segmentation in the time domain. In this way,

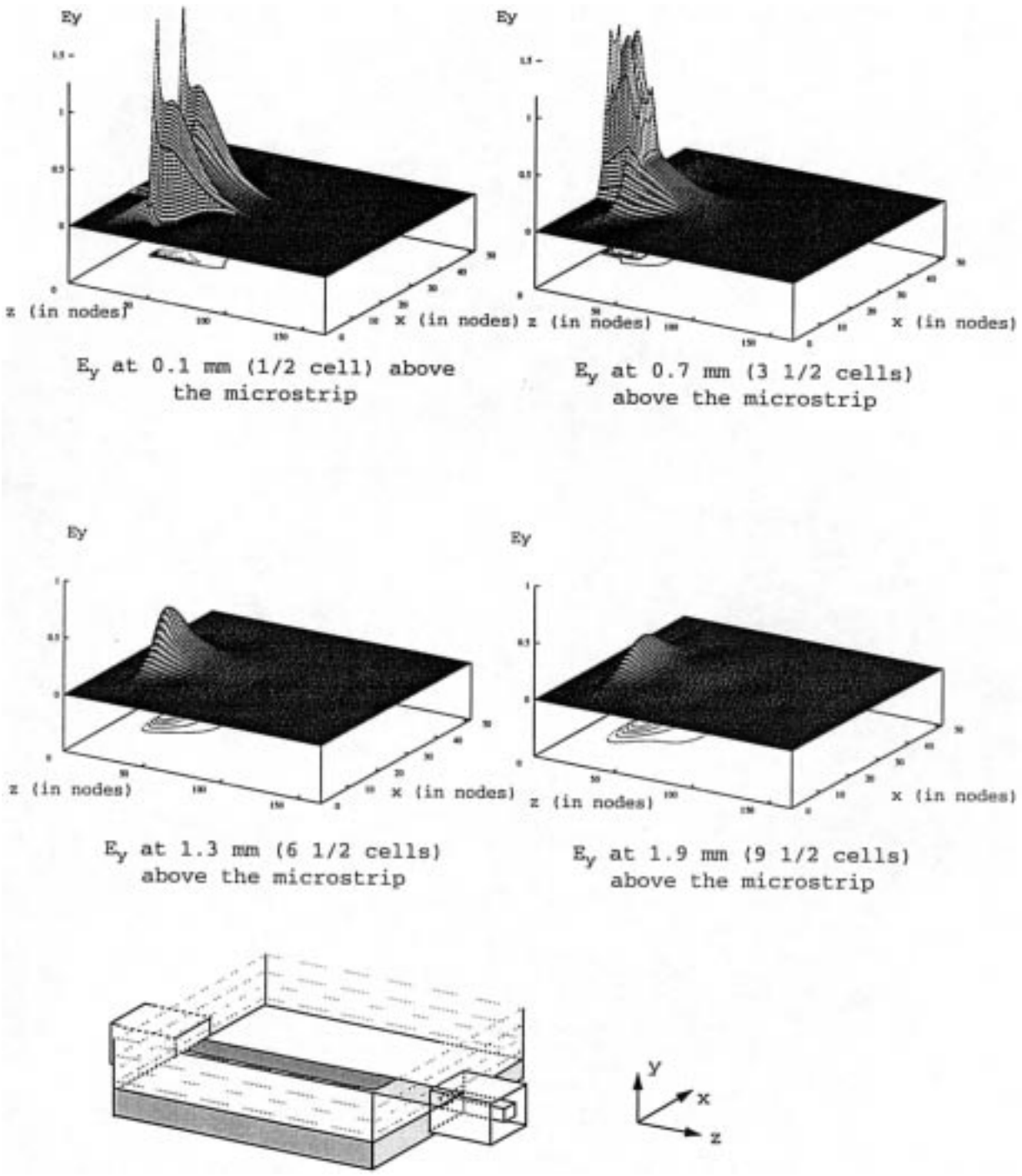

Fig. 8. E_y field at time-step 200 (when the Gaussian pulse enters the microstrip circuit) at different distances from the surface of the microstrip.

the efficiency of a modal approach and the capabilities of a time-domain method are combined.

VI. Numerical Results

The packaged microstrip via-hole has been discretized with a uniform TLM mesh of size $\Delta l = 0.2$ mm. A simulation has been performed for the full and segmented structure terminated with modal short-circuit BC's (SBC). The SBC's have been placed at one-third of the box depth, confining the standard TLM mesh to the complex region comprising the coax-to-microstrip transitions and the planar circuit. The TLM computational volume is, therefore, reduced by a factor of three. The feature nearest to the SBC's is the microstrip-to-coax transition which is just five cells away. The time-domain waveforms at the input and output coaxial ports in the two situations are shown in Fig. 5.

The two time-domain waveforms overlap, thus confirming the accuracy of the modal SBC. After the main pulse has reached the coaxial ports, the field inside the package keeps ringing for a very long time. The metallic box behaves like a

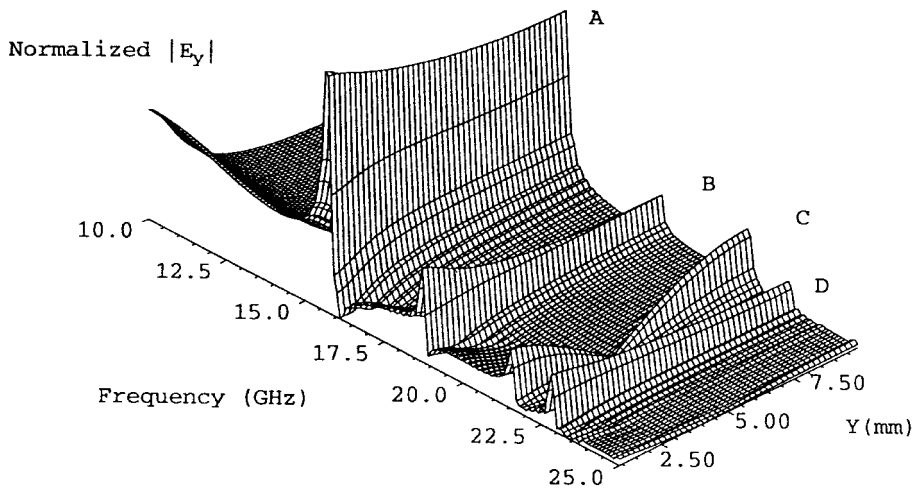

Fig. 9. Variation of the steady state E_y field with frequency and height above the via.

high-quality resonator from which the energy is slowly drained through the two coaxial ports.

A large number of time steps is, therefore, necessary to accurately characterize the resonance effect. In this case, the simulation has been extended to 16 000 time steps to obtain a negligible Gibbs' error due to the truncation of the time-domain waveforms. The corresponding S-parameters obtained with the full and the segmented domain simulations using the above time-domain waveforms are shown in Fig. 6.

The results obtained with the hybrid approach (whether numerically or analytically generated modal Green's functions) overlap those obtained with a full TLM simulation of the problem. The comparison with the measurements performed in [6] validates the approach. Note that the resonances are fully predicted since they are related to the package dimensions. The difference in the transmission coefficient visible at lower frequencies is believed to be due to the square coaxial line used in the simulation instead of the round coaxial line used in the measurements. Nevertheless, the overall agreement is excellent.

In the TLM simulation of the segmented structure, all of the modes excited by the structure up to the TE^y_{43} and TM^y_{43} have been considered in the terminating conditions. The comparison of mesh size and central processing unit (CPU) time on a 100-MHz HP-735 workstation for the two TLM analyses is summarized in Table I. The modal boundary treatment alone requires 10 min, which is equivalent to a layer of about four TLM nodes above the microstrip in the package. This load could be reduced by exploiting a more efficient modal analysis and synthesis.

The TLM model exploits symmetry about the center of the structure and separate meshes (each of $5 \times 10 \times 25$ nodes) have been used for the input and the output feeds. These feeds have been modeled with square coaxial cross section of 10×10 nodes with a 4×4 nodes inner conductor giving a characteristic impedance of 50 Ω. The feeds have been terminated on single reflection-coefficient BC $\Gamma = 0$ matching the outgoing TEM waves. The microstrip width is 2.4 mm, giving a characteristic impedance of 50.5 Ω. The coax-to-microstrip transition is realized by extending the center conductor 1.6 mm into the package and connecting it vertically. The strip is longitudinally indented by 0.2 mm to avoid contact with the package walls. An edge correction [22] is often required in simulations of microstrip circuits but it has no significant effect here, as the sharp features in the response are dictated by the package. In the segmented domain, the length of the Green's function was 2000 time steps. Note that both memory and CPU time are significantly reduced when the hybrid approach is used.

The package is a highly resonant structure where the stability of the BC's is heavily tested. Resonating structures are, in fact, among the most critical structures for which to generate BC's, and long-term stability may be difficult to achieve [23]. Instabilities have been recently reported for BC's placed parallel to the main propagation direction of the wave [24]. However, during simulations with modal diakoptics, we have never encountered instabilities, neither with analytical nor with TLM-generated Green's functions. The stability of the SBC is a critical factor in the simulation of resonant structures, especially when active elements are included in the planar circuit.

To further test the stability of the SBC, the number of modes has been reduced to the first three modes excited in the package (TM^y_{01}, TE^y_{11}, and TM^y_{11}). Surprisingly, the simulation always remained stable. The surprise resides in the fact that by reducing the number of modes in the SBC's, causality in the circuit may be violated. In fact, by reinjecting the reflected field composed of only a few modes in the computational domain, some energy may reach the output port of the structure *before* the main wave propagating along the microstrip does. Stability may be due to the fact that the modes not included in the SBC are incidentally matched by the characteristic impedance of the TLM link lines. This termination, although not a rigorous termination for the modes, behaves mainly as an ABC. The S-parameters obtained with only the first three modes in the SBC are shown in Fig. 7.

Note that the resonance due to the modes with order "21" has been lost. This resonance has been numerically suppressed

by eliminating the corresponding Green's function. It also appears that the package (its cutoff frequency occurs at 6 GHz) supports several resonant frequencies up to 20 GHz (operating frequency range of the planar circuit). Among the possible resonant modes only two (the "11" and "21" modes) couple to the microstrip circuit by virtue of symmetry. These results show that the number of modes is important since too few of them may lead to stable, but wrong, results.

In order to visualize how the higher order modes decay away form the surface of the microstrip, the E_y field component has been plotted at several distances above the surface of the strip at an instant in time (Fig. 8).

Note that the singular fields at the microstrip edges quickly decay when the sampling plane moves away from the strip. At 1.9 mm above the surface of the planar circuit, the field is still complex but amenable to an expansion into a relatively small number of modes.

In order to confirm that modal diakoptics applied along a plane parallel to the propagation direction of the field in the microstrip actually correctly matches all the resonances, the steady-state field variation with frequency along a y-directed line placed adjacent to the via (obtained from the full structure) has been plotted in Fig. 9.

Away from the resonant frequency the field tends to exponentially decay away from the strip. It is then possible to clearly recognize four resonances in the range from dc to 25 GHz, labeled A, B, C, and D with different characteristics. Resonance A (at 15.6 GHz) has a "11" variations in the x–z plane and has no sin-type variations with respect to y. Whereas, resonance B (at 21.5 GHz) exhibits a half-cycle in y. Such plots can be used to identify package modes which interfere with the correct operation of the circuit.

The fact that the results obtained with the hybrid approach identifies all of the resonances clearly shows that the SBC's accommodate modes with arbitrary orientation.

VII. Conclusion

Hybrid approaches combine the features of different methods to produce a more efficient and *smart* solution of electromagnetic problems. By combining TLM for modeling the more irregular sub-volumes with modal characterization of homogenous sub-volumes, we have been able to model a typical packaged component with less than half the computing resources. In addition, the modal approach sheds some light onto the physics of the packaged resonances, thus helping the designer to develop better packages. For the optimization of the package size, for example, it is straightforward to analytically generate the modal Green's functions for a modified package and to interface them with the planar circuit. Comparison with measurements available in the literature validate the approach.

References

[1] Special issue, *IEEE Trans. Microwave Theory Tech.*, vol. 42, Sept. 1994.

[2] R. Faraji-Dana and Y. L. Chow, "A CAD tool for interference rejection of a microwave circuit making use of resonance of the circuit packaging," in *IEEE MTT-S Int. Microwave Symp. Dig.*, San Diego, CA, May 1994, pp. 1523–1526.

[3] P. B. Johns, "A symmetrical condensed node for the TLM method," *IEEE Trans. Microwave Theory Tech.*, vol. MTT-35, pp. 370–377, Apr. 1987.

[4] K. S. Yee, "Numerical solutions of initial boundary value problems involving Maxwell's equations in isotropic media," *IEEE Trans. Antennas Propagat.*, vol. AP-14, pp. 302–307, May 1966.

[5] M. Righi, "Diakoptics solution techniques for electromagnetic fields in time and frequency domain," Ph.D. dissertation, Dept. Elect. Comput. Eng., Univ. Victoria, Victoria, B.C., Canada, 1995.

[6] P. Mezzanotte, M. Mongiardo, L. Roselli, R. Sorrentino, and W. Heinrich, "Analysis of packaged microwave integrated circuits by FDTD," *IEEE Trans. Microwave Theory Tech.*, vol. 42, pp. 1796–1801, Sept. 1994.

[7] M. Righi and W. J. R. Hoefer, "Modal Johns matrices for waveguide components," in *Proc. 1st Int. Workshop Transmission Line Modeling (TLM)*, Victoria, B.C., Canada, Aug. 1–3, 1995, pp. 233–236.

[8] ———, "Efficient hybrid TLM/mode-matching analysis of packaged components," in *IEEE MTT-S Int. Microwave Symp. Dig.*, San Francisco, CA, June 1996, pp. 447–450.

[9] F. Alimenti, P. Mezzanotte, L. Roselli, and R. Sorrentino, "Analysis of planar circuits with a combined 3-D FDTD-time-domain modal expansion method," in *IEEE MTT-S Int. Microwave Symp. Dig.*, San Francisco, CA, June 1996, pp. 1471–1474.

[10] C. Eswarappa, G. I. Costache, and W. J. R. Hoefer, "TLM modeling of dispersive wide-band absorbing boundaries with time-domain diakoptics for S-parameter extraction," *IEEE Trans. Microwave Theory Tech.*, vol. 38, pp. 379–386, Apr. 1990.

[11] M. Righi, M. Mongiardo, R. Sorrentino, and W. J. R. Hoefer, "Efficient TLM diakoptics for separable structures," in *IEEE MTT-S Int. Microwave Symp. Dig.*, Atlanta, GA, June 1993, pp. 425–428.

[12] F. Moglie, T. Rozzi, P. Marcozzi, and A. Schiavoni, "A new termination condition for the application of FDTD techniques to discontinuity problems in close homogenous waveguides," *IEEE Microwave Guided Wave Lett.*, vol. 2, pp. 475–477, Dec. 1992.

[13] T. W. Huang, B. Houshmand, and T. Itoh, "Efficient modes extraction and numerically exact matched sources for a homogenous waveguide cross section in a FDTD simulation," in *IEEE MTT-S Int. Microwave Symp. Dig.*, San Diego, CA, May 1994, pp. 31–33.

[14] E. Tentzeris, M. Krumpholtz, N. Dib, and L. P. B. Katehi, "A waveguide absorber based on analytical Green's functions," in *25th European Microwave Conf.*, Bologna, Italy, Sept. 1995, pp. 251–254.

[15] F. Alimenti, P. Mezzanotte, L. Roselli, and R. Sorrentino, "Efficient analysis of waveguide components by FDTD combined with time-domain modal expansion," *IEEE Microwave Guided Wave Lett.*, vol. 5, pp. 351–353, Oct. 1995.

[16] M. Righi and W. J. R. Hoefer, "Efficient 3-D SCN–TLM diakoptics for waveguide components," *IEEE Trans. Microwave Theory Tech.*, vol. 42, pp. 2381–2385, Dec. 1994.

[17] M. Mongiardo, M. Righi, R. Sorrentino, and W. J. R. Hoefer, "Rigorous and fast computation of modal Johns response," presented at the *Proc. 2nd Int. Workshop Discrete Time-Domain Modeling Electromagnetic Fields Network*, Berlin, Germany, Oct. 1993.

[18] Z. Chen, W. J. R Hoefer, and M. M. Ney, "A new procedure for interfacing the transmission line matrix method with frequency domain solutions," *IEEE Trans. Microwave Theory Tech.*, vol. 38, pp. 1788–1792, Oct. 1991.

[19] C. Fuchs, G. Kopp, and A. J. Schwab, "An efficient algorithm for computing the transmission through highly conducting thin shields in TLM," *Int. J. Numer. Modeling, Electron. Networks, Devices, Fields*, vol. 8, no 5, pp. 331–340, Sept./Oct. 1995.

[20] Z. Bi, K. Wu, and J. Litva, "Designing dispersive boundary condition (DBC) for the FDTD method using digital filtering theory," *IEEE Antennas Propagat. Symp. Dig.*, Chicago, IL, July 1992, pp. 326–329.

[21] P. Russer, M. Righi, C. Eswarappa, and W. J. R. Hoefer, "Lumped element equivalent circuit parameter extraction of distributed microwave circuits via TLM simulation," in *IEEE MTT-S Int. Microwave Symp. Dig.*, San Diego, CA, May 1994, pp. 887–890.

[22] J. L. Herring and W. J. R. Hoefer, "Compensation of coarseness error in TLM modeling of microwave structures with the symmetrical condensed node," in *IEEE MTT-S Int. Microwave Symp. Dig.*, Orlando, FL, May 1995, pp. 23–26.

[23] C. Eswarappa and W. J. R. Hoefer, "One way equation absorbing boundary conditions for 3-D TLM analysis of planar and quasi-planar structures," *IEEE Trans. Microwave Theory Tech.*, vol. 42, pp. 1669–1677, Sept. 1994.

[24] M. Krumpholz, B. Bader, and P. Russer, "On the theory of discrete TLM Green's function in three-dimensional TLM," *IEEE Trans. Microwave Theory Tech.*, vol. 43, pp. 1472–1483, July 1995.

Mario Righi (S'91–M'91) was born in Perugia, Italy. He received the Laurea degree (summa cum laude) in electronic engineering from the University of Ancona, Ancona, Italy, in 1991, and the Ph.D. degree in electrical engineering from the University of Victoria, Victoria, B.C., Canada, in 1995.

He is currently a Research Engineer at the University of Victoria. His research interest is in the use of hybrid methods in computational electromagnetics.

Dr. Righi was awarded the IEEE Graduate Student Fellowship Award from the IEEE Microwave Theory and Techniques Society in 1993, the Quality Presentation Recognition Award in 1994, and an NSERC Post-Doctoral Fellowship by the Natural Sciences and Engineering Research Council of Canada in 1995.

Jonathan L. Herring was born in Middlesbrough, U.K., in 1966. He received the M.Eng. degree in electrical and electronic engineering and the Ph.D. degree from the University of Nottingham, Nottingham, U.K., in 1989 and 1993, respectively.

From 1989 to 1993, he was employed as a Research Assistant at the University of Nottingham, where he worked on the modeling of EMC problems using the TLM technique. From 1993 to 1996, he was with the Department of Electrical and Computer Engineering, University of Victoria, B.C., Canada, working as a Post-Doctoral Fellow. He is currently a Software Engineer at Schumberger GeoQuest, Abingdon, U.K.

Wolfgang J. R. Hoefer (M'71–SM'78–F'91) received the Dipl.-Ing. degree in electrical engineering from the Technische Hochschule Aachen, Aachen, Germany, in 1965, and the D.Ing. degree from the University of Grenoble, Grenoble, France, in 1968.

In 1969, he joined the Department of Electrical Engineering, University of Ottawa, Ottawa, Ont., Canada, where he was a Professor until 1992. Since 1992, he has held the NSERC/MPR Teltech Industrial Research Chair in RF engineering in the Department of Electrical and Computer Engineering, University of Victoria, B.C., Canada, and is a Fellow of the Advanced Systems Institute of British Columbia. During two sabbatical leaves, he worked with the Space Division of AEG-Telefunken, Backnang, Germany (now ATN), and with the Electromagnetics Laboratory of the Institut National Polytechnique de Grenoble, France, in 1976 and 1977, respectively. During 1984 and 1985, he has been a Visiting Scientist at the Space Electronics Directorate of the Communications Research Centre, Ottawa, Canada. From 1990 to 1991, he spent a third sabbatical year as a Visiting Professor at the Universities of Rome "Tor Vergata" in Italy, Nice–Sophia Antipolis in France, and Munich (TUM) in Germany. His research interests include numerical techniques for modeling electromagnetic fields and waves, computer-aided design of microwave and millimeter-wave circuits, microwave measurement techniques, and engineering education.

Dr. Hoefer is the co-founder and managing editor of the *International Journal of Numerical Modeling*.